Nitrofurantoin–*p*-Aminobenzoic Acid Cocrystal: Hydration Stability and Dissolution Rate Studies

SURYANARAYAN CHERUKUVADA, N. JAGADEESH BABU, ASHWINI NANGIA

School of Chemistry, University of Hyderabad, Prof. C. R. Rao Road, Gachibowli, Hyderabad 500046, Andhra Pradesh, India

Received 20 October 2010; revised 10 January 2011; accepted 23 February 2011

Published online 18 March 2011 in Wiley Online Library (wileyonlinelibrary.com). DOI 10.1002/jps.22546

ABSTRACT: Nitrofurantoin (NF) drug is known to transform to a hydrate form in aqueous medium. The hydration stability and dissolution rate of a few cocrystals of NF were compared with that of its stable β polymorph and hydrate form II. Hydrogen bonding and molecular packing in the novel cocrystal structures were analyzed. Pharmaceutical cocrystals of NF with *p*-aminobenzoic acid (PABA) and urea showed superior physicochemical properties compared with the known L-arginine salt hydrate. All the solid-state adducts were characterized by single-crystal X-ray diffraction, X-ray powder diffraction, differential scanning calorimetry, and thermogravimetric analysis. NF–PABA cocrystal was found to be superior among the compounds studied in terms of minimal transformation to NF hydrate and comparable dissolution rate to the reference drug. © 2011 Wiley-Liss, Inc. and the American Pharmacists Association J Pharm Sci 100:3233–3244, 2011

Keywords: antibacterial; co-crystal; hydration; intrinsic dissolution rate; nitrofurantoin; polymorph; solubility; stability; transformation; X-ray diffractometry.

INTRODUCTION

Nitrofurantoin (NF) is an antibacterial drug used for the treatment of urinary tract infections.[1] This drug is on the WHO Model List of Essential Medicines.[2] Polymorphism and pseudopolymorphism of NF are reported in the literature.[3,4] There are two polymorphs of anhydrous NF (α and β),[5] two polymorphs of NF monohydrate (Form I and Form II),[6] and two pseudopolymorphs of the drug with dimethylformamide and dimethyl sulfoxide (designated as Form III and Form IV).[7] NF (Fig. 1) is a Class IV drug[8] according to the Biopharmaceutics Classification System, that is, it has low solubility and low permeability (and bioavailability). A common side effect of NF is nausea and emesis due to its high absorption rate immediately after oral administration.[9] The same study[9] reported that larger crystals (150 μm mesh size) of lower surface area and slower absorption reduce emesis side effect, and still confer optimal therapeutic impact. The drug is marketed as macrocrystalline NF (brand name Macrodantin - Pfizer Australia Pty Ltd., West Ryde, New South Wales, Australia).[1,10] The reference drug is the stable β polymorph.[11] The dissolution profile of the drug is variable; after a high initial dissolution, the drug is released slowly because it converts to the more stable monohydrate II in an aqueous medium, and it is the latter form that has lower dissolution rate.[7] The transformation of NF anhydrate to monohydrate was observed during dissolution,[4,7] pelletization,[12] and granulation.[13] Dehydration kinetics of the monohydrate[14] and solution behavior of NF anhydrate and monohydrate have been studied.[15] Nitrofurantoin salts with sodium and potassium[16] and L-arginine, L-lysine, L-histidine, L-ornithine, and glycine[17] are known in the patent literature.The cocrystallization approach is attracting an immense interest from pharmaceutical scientists to control the physicochemical properties of drugs such as solubility, dissolution, hydration, stability, compaction, tableting, and so on.[18–22] We prepared cocrystals of NF with coformers of complementary functional groups (see Fig. 1) to control the spontaneous hydration and solubility/dissolution of the drug. A control over the dissolution rate can influence the absorption rate, which in turn may regulate the side effects of the drug.

Additional Supporting Information may be found in the online version of this article. Supporting Information

Correspondence to: Ashwini Nangia (Telephone: +91-40-23134854; Fax: +91-40-23010567; E-mail: ashwini.nangia@gmail.com)

Journal of Pharmaceutical Sciences, Vol. 100, 3233–3244 (2011)

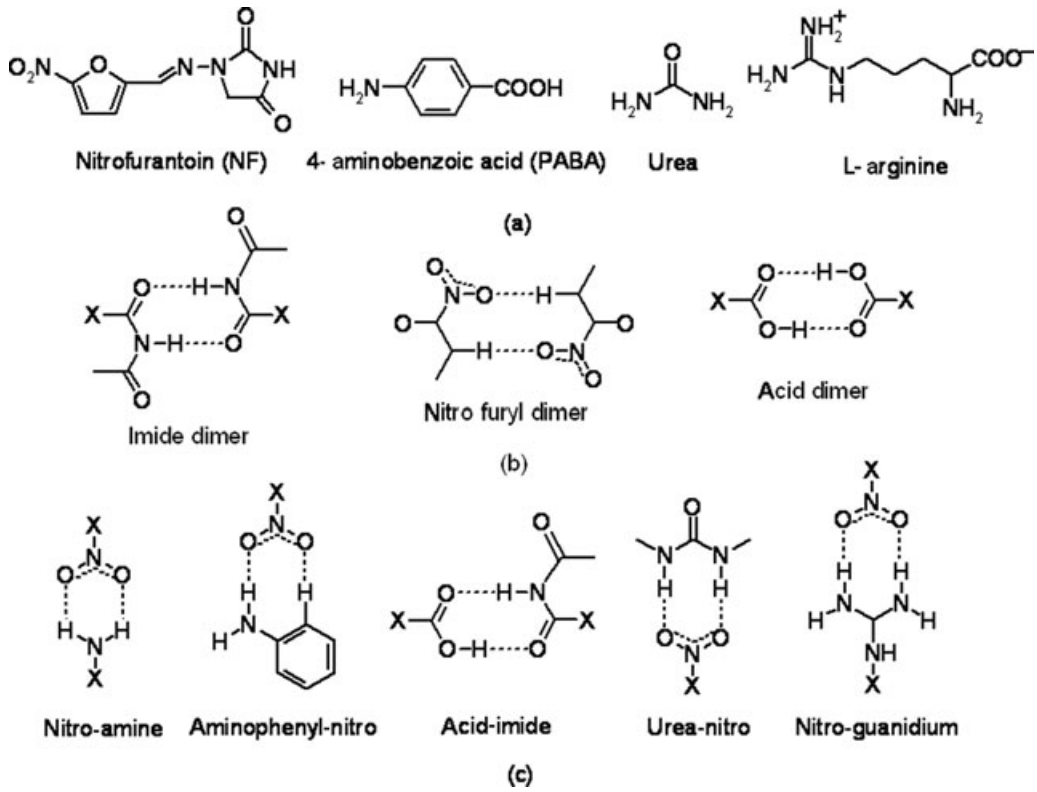

Figure 1. (a) Molecular structure of nitrofurantoin and coformers used in this study. (a) Some possible homosynthons (b) and heterosynthons (c) between the molecular components in the cocrystal.

RESULTS AND DISCUSSION

Commercially available NF [Alfa Aesar material matched with the known β form, X-ray powder diffraction (XRPD) plot in Fig. S1, Supporting Information] was used in all our experiments. Cocrystallization of NF with coformers such as *p*-aminobenzoic acid (PABA), urea, and L-arginine was attempted on the basis of the potential heterosynthons[23,24] shown in Figure 1. Two 1:1 NF–PABA and NF–urea cocrystals and a 1:1:1 NF–L-arginine–H_2O salt were obtained and characterized (see *Experimental* section). A NF–methanol (MeOH) solvate was also crystallized during our experiments. X-ray crystallographic parameters are shown in Table 1, and hydrogen bonds are shown in Table 2.

Cocrystal of NF and PABA

A 1:1 cocrystal of NF–PABA was obtained when an equimolar mixture of the two components were dissolved in acetonitrile. NF molecules are hydrogen bonded via the imide dimer, and PABA molecules are connected via the acid dimer homosynthons[24] (see Fig. 1). Such dimeric units are connected via the N-H···O + C-H···O two-point aminophenyl–nitro motif as zigzag tapes. Two-dimensional sheets are sustained by auxiliary C-H···O interactions (Fig. 2), which lie at an interplanar separation of 3.6 Å. An alternative crystal structure of this cocrystal was anticipated with acid–imide heterosynthon (Fig. 1) between NF and PABA, but such a structure was not realized experimentally. Solid-state grinding[25] of the components in equimolar stoichiometry resulted in the same cocrystal. This cocrystal was found to be stable to slurry crystallization in water, suggesting that it is a stable form.

Cocrystal of NF and Urea

A 1:1 cocrystal of NF and urea was obtained when an equimolar mixture of the components was subjected to solid-state grinding. Single crystals suitable for X-ray diffraction were obtained from DMF−dioxane solvent mixture. There is no two-point urea–nitro synthon in this crystal structure. A linear tape of nitrofuryl C-H···O dimers of NF molecules is connected through N-H···O hydrogen bonds to the urea dimer (Fig. 3).

Hydrate of NF and L-arginine Salt

A salt of NF and L-arginine with a solvent of crystallization was reported in a patent.[17] We obtained a 1:1:1 NF–L-arginine–H_2O salt crystal when an equimolar mixture of NF and L-arginine was crystallized from acetonitrile–isopropanol solvent mixture.

 DOI 10.1002/jps

Table 1. Crystallographic Parameters of the Multicomponent Adducts

Molecular Complex	NF–PABA	NF–Urea	NF–L-Arginine–H_2O	NF–MeOH
Empirical formula	$(C_8H_6N_4O_5)$–$(C_7H_7NO_2)$	$(C_8H_6N_4O_5)$–(CH_4N_2O)	$(C_8H_6N_4O_5)$–$(C_6H_{15}N_4O_2)$–(H_2O)	$(C_8H_6N_4O_5)$–(CH_4O)
Formula weight	375.30	298.23	430.40	270.21
Crystal system	Triclinic	Monoclinic	Orthorhombic	Monoclinic
Space group	$P\bar{1}$	$P2_1/n$	$P2_12_12_1$	$P2_1/c$
T/K	298(2)	100(2)	100(2)	298(2)
a/Å	6.7239(11)	6.681(3)	5.7872(6)	6.4279(17)
b/Å	7.5460(12)	13.653(6)	15.3731(16)	6.7824(18)
c/Å	16.316(3)	13.189(6)	21.173(2)	26.841(7)
$\alpha/^\circ$	93.827(2)	90	90	90
$\beta/^\circ$	92.538(2)	97.460(7)	90	92.149(4)
$\gamma/^\circ$	101.659(2)	90	90	90
Z	2	4	4	4
V/Å^3	807.5(2)	1192.9(9)	1883.7(3)	1169.4(5)
D_{calc}/g cm^{-3}	1.543	1.661	1.518	1.535
μ/mm^{-1}	0.125	0.142	0.126	0.131
Reflns collected	8466	10368	19511	11753
Unique reflns	3191	2130	3679	2335
Observed reflns	2722	1821	3476	1897
$R_1[I > 2\sigma(I)]$	0.0382	0.0539	0.0336	0.0429
wR_2 [all]	0.0985	0.1430	0.0789	0.1134
Goodness-of-fit	1.054	1.049	1.047	1.039

Solid-state grinding of the components (to avoid contact with water/moisture) did not afford an anhydrous salt as monitored by XRPD. Water-assisted grinding[26] of the components resulted in the same salt hydrate, and this method was used to prepare the material reproducibly. Attempts to dehydrate the salt hydrate did not succeed as the material decomposed abruptly around 180°C as monitored by differential scanning calorimetry (DSC) (exotherm) and thermogravimetric analysis (TGA) (weight loss) (Fig. 4). The measured weight loss of 27% in TGA [and thermogravimetry (TG)–mass spectrometry (MS), see Fig. S2, Supporting Information] corresponds to the theoretical loss of four volatile components from the salt hydrate—CO_2, H_2O, NH_3, and NO_2 (calculated 29.04%). The elemental analysis of the decomposed material showed C 51.12%, H 5.82%, N 27.35%, and O 15.71% (remaining), which matches with the empirical formula $C_{13}H_{18}N_6O_3$ that can be obtained by the loss of the above volatile components. It seems that the molecular complex is not stable without a solvent of crystallization. In the crystal structure, the imine proton of NF is transferred to the α-amino group of L-arginine. There is no two-point nitroguanidium synthon (Fig. 1) between NF and L-arginine molecules but instead N-H···O and N-H···N hydrogen bonds assemble as a zigzag tape (Fig. 5). The tapes are arranged in a herringbone T motif that makes channels for water inclusion along the *a*-axis.

NF Methanolate

A 1:1 MeOH solvate (NF–MeOH) was crystallized from MeOH. The crystals turned opaque after complete evaporation of the solvent and slowly converted to NF monohydrate Form II at ambient temperature and humidity as monitored by XRPD (Fig. S3, Supporting Information). Guest exchange of NF–MeOH with water was instant as the crystals opaqued immediately when suspended in water and converted to monohydrate II. DSC of NF methanolate showed an endotherm at 105°C prior to melting and decomposition (270°C), which is due to desolvation of MeOH as observed from the weight loss of the material in TGA (experimental 11.83% and calculated 11.85% for 1 mol of MeOH) (Fig. 6). Controlled desolvation of NF methanolate at 125°C for 1 h resulted in a powdery material whose XRPD pattern matched with that of NF β polymorph (Fig. S4, Supporting Information). In the crystal structure of NF–MeOH, a tape of NF molecules assembled via C-H···O interactions connects to MeOH molecules through O_{MeOH}-H···O_{NF} hydrogen bond. The tapes of NF molecules form a herringbone motif such that the channels of MeOH molecules are parallel to the *b*-axis (Fig. 7). The channel structure of NF methanolate is a reason for its low stability and facile transformation to the hydrate form. There are no apparent similarities between the methanolate and hydrate II crystal structures except that the guest molecules reside in channel/cavity along the *b*-axis in both structures.

Equilibrium Solubility and Intrinsic Dissolution Rate

Nitrofurantoin is a low water solubility drug with values reported that are quite far apart of 80 mg/L[7] and 190 mg/L[17] at 25°C. We measured the equilibrium solubility of NF at ambient temperature and humidity, and our value (82 mg/L) matches with the

Table 2. Hydrogen Bonds in Crystal Structures of the Molecular Complexes

Interaction	H···A/Å	D···A/Å	∠D–H···A/°	Symmetry Code
NF—PABA				
N4–H4···O5	1.83	2.827(2)	165.3	$-x, 1-y, 1-z$
N5–H5A···O4	2.44	3.204(2)	131.5	$1+x, y, z$
N5–H5B···O3	2.25	3.265(2)	176.3	$1-x, 2-y, 2-z$
N5–H5A···O2	2.70	3.424(2)	128.9	$1-x, 1-y, 1-z$
O7–H7···O6	1.60	2.589(2)	178.4	$-x, -y, 1-z$
C3–H3···O4	2.50	3.263(2)	126.3	$1+x, y, z$
C5–H5···O4	2.30	3.157(2)	134.1	$1+x, y, z$
C14–H14···O2	2.35	3.381(2)	158.1	$1-x, 2-y, 2-z$
C8–H8B···O6	2.61	3.615(2)	153.2	$1-x, 1-y, 1-z$
NF—urea				
N4–H4···O6	1.74	2.724(3)	163.1	$1/2-x, 1/2+y, 1/2-z$
N5–H5A···O3	2.23	3.144(3)	148.9	$x, y, 1+z$
N5–H5B···O4	2.15	3.062(3)	148.5	$x, y, 1+z$
N5–H5B···N2	2.49	3.308(3)	137.1	$x, y, 1+z$
N6–H6A···O6	1.95	2.960(3)	178.4	$-x, 1-y, 1-z$
N6–H6B···O4	2.19	3.071(3)	144.1	x, y, 1+z
N6–H6B···O5	2.50	3.023(3)	111.1	−1/2+x, 3/2−y, 1/2+z
N5–H5A···O1	2.59	3.188(3)	117.4	$x, y, -1+z$
C2–H2···O2	2.39	3.264(3)	136.4	$-x, -y, -z$
C3–H3···O5	2.35	3.355(3)	152.9	$1/2-x, -1/2+y, 1/2-z$
C5–H5···O3	2.52	3.181(3)	118.2	$1/2+x, 1/2-y, 1/2+z$
C5–H5···O2	2.60	3.668(3)	167.4	$1/2+x, 1/2-y, 1/2+z$
C3–H3···O3	2.62	3.216(3)	113.7	$1/2+x, 1/2-y, 1/2+z$
C8–H8A···O4	2.70	3.650(3)	146.1	$1-x, 1-y, -z$
NF —L-arginine—H_2O				
N5–H5A···O5	1.78	2.775(2)	167.7	$x, -1+y, z$
N5–H5B···O8	2.01	2.880(2)	141.7	$x, -1+y, -1+z$
N5–H5C···O6	1.66	2.670(2)	176.1	$1+x, y, z$
N6–H6···N4	2.03	3.030(2)	167.7	$-x, -1/2+y, 1/2-z$
N7–H7A···O5	1.87	2.874(2)	169.4	$-x, -1/2+y, 1/2-z$
N7–H7B···O4	1.75	2.755(2)	172.4	$1/2+x, 1/2-y, 1-z$
N8–H9A···O3	2.06	3.062(2)	167.4	$1/2+x, 1/2-y, 1-z$
N8–H9B···N2	2.35	3.342(2)	164.1	$1/2+x, 1/2-y, 1-z$
O8–H15A···O7	1.86	2.836(2)	167.2	$1+x, 1+y, 1+z$
O8–H15B···O7	1.86	2.830(2)	164.5	$1/2+x, 1/2-y, 1-z$
C3–H3···O6	2.49	3.075(2)	112.2	$3/2+x, 1/2-y, -z$
C12–H12B···O6	2.50	3.281(2)	128.0	$1+x, y, z$
C2–H2···O2	2.51	3.589(2)	169.6	$1/2+x, 1/2-y, -z$
C2–H2···O3	2.57	3.340(2)	127.0	$1/2+x, 1/2-y, 1-z$
C13–H13B···O2	2.67	3.582(2)	141.5	$1+x, y, z$
C3–H3···O7	2.49	3.525(2)	158.5	$3/2+x, 1/2-y, -z$
C5–H5···O8	2.47	3.429(2)	146.0	$1/2+x, 3/2-y, 1-z$
C8–H8A···O7	2.64	3.636(2)	152.2	$1/2+x, 1/2-y, -z$
C11–H11A···O4	2.65	3.203(2)	110.7	$-x, 1/2+y, 1/2-z$
C11–H11A···O4	2.58	3.323(2)	124.8	$x, -1+y, z$
NF—MeOH				
N4–H4···O6	1.77	2.777(2)	172.7	$-x, 1/2+y, 3/2-z$
O6–H6···O5	1.83	2.809(2)	174.0	$1-x, -1/2+y, 3/2-z$
C2–H2···O3	2.35	3.230(2)	137.1	$1+x, y, z$
C5–H5···O4	2.11	3.171(2)	164.5	$1+x, y, z$
C8–H8B···O6	2.60	3.656(2)	165.7	$1+x, y, z$
C9–H9A···O4	2.71	3.501(2)	129.2	$1+x, y, z$

O–H, N–H, and C–H distances are neutron-normalized to 0.983, 1.009, and 1.083 Å, respectively.
NF, nitrofurantoin; PABA, *p*-aminobenzoic acid.

lower number. Caira et al.[7] have suggested that anhydrous NF (commercial NF β polymorph of this study) transforms to monohydrate II and hence the measured solubility of anhydrous NF is actually that of the monohydrate II. This transformation means that NF monohydrate II is more stable than the anhydrate β polymorph in water at 25°C. The above transformation was monitored by XRPD of the undissolved drug after the solubility experiment at 24 h in our experiments.

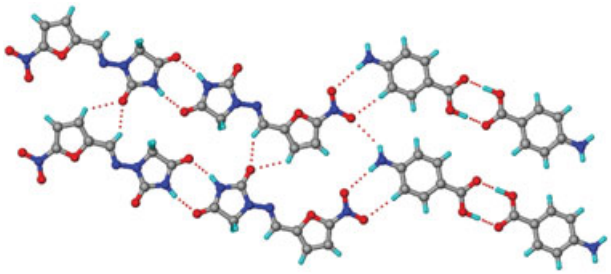

Figure 2. Nitrofurantoin and *p*-aminobenzoic acid molecules are hydrogen bonded via imide dimer and acid dimer homosynthons, which are in turn connected by aminophenyl–nitro N-H···O and C-H···O bonds to form zigzag tapes, which are connected through bifurcated C-H···O interactions to make a sheet structure.

The aqueous solubility of NF–PABA, NF–urea, and NF–L-arginine–H_2O was measured at 25°C. We were able to obtain the value for NF–PABA cocrystal only (the value of 216 mg/L is the molar equivalent solubility of NF in the cocrystal) because the other two compounds transformed to NF monohydrate II within 1 h of the solubility experiment (analyzed by XRPD of the undissolved residue). The XRPD of the undissolved material from the solubility experiment of NF–PABA did not show any transformation to any of the NF forms (polymorph or hydrate), meaning that the cocrystal is quite stable (Fig. 8). When PABA was added to NF as an additive from 5% to 60% by weight in water slurry and the residue analyzed by XRPD

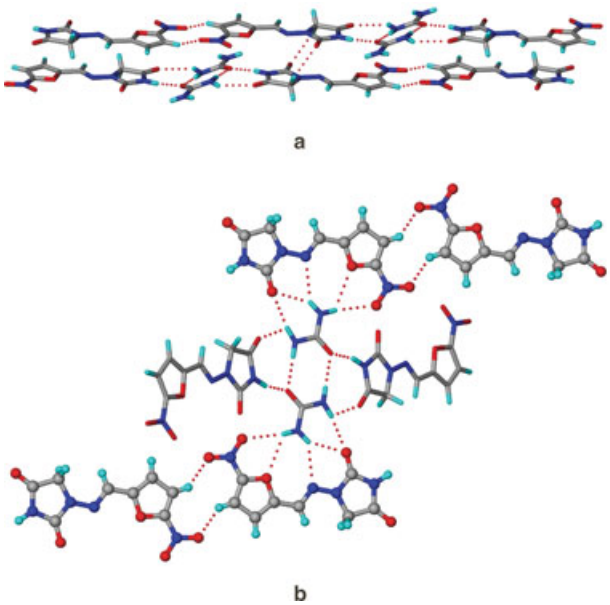

Figure 3. (a) Parallel tapes of nitrofuryl C-H···O dimers of nitrofurantoin molecules are connected through N-H···O bonds to the urea dimer. The offset tapes are connected via a C-H···O interaction. (b) Adjacent tapes (shown as ball-stick and capped-stick models for clarity) along *c*-axis make an angle of 28.2° with each other.

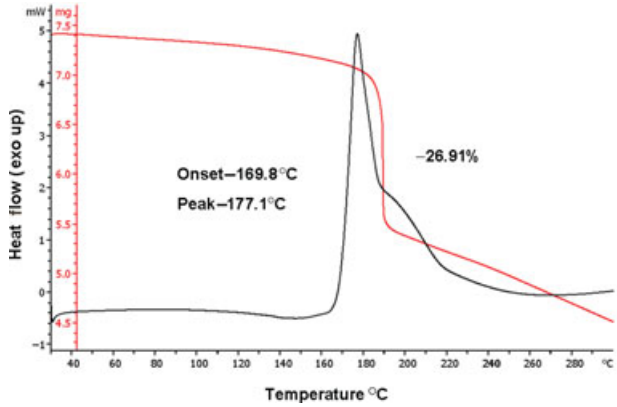

Figure 4. Differential scanning calorimetry (black trace) and thermogravimetric analysis (red trace) of NF–L-arginine–H_2O.

(Table 3), there is no effect of PABA additive in reducing the hydration of the drug in water. With increasing concentration of PABA, there is a decrease in the proportion of NF monohydrate II in the residue, which means that PABA reacted with NF to form the stable cocrystal in solution. Complexation between NF and PABA was observed by a visible color change of the solution from yellow to orange, while the unreacted NF transformed to the monohydrate (Fig. 9). Only at 57.6% of PABA-to-NF ratio (which is the molar proportion of the components in the 1:1 NF–PABA cocrystal), the material was found to be stable to hydration. This means that PABA was effective as a coformer in molar stoichiometry in the 1:1 cocrystal composition to make NF stable to hydration.

The intrinsic dissolution rates (IDRs) of NF β polymorph, NF monohydrate II, NF–PABA, NF–urea, and NF–L-arginine–H_2O were measured in three different media, pure water (pH 6.4), 0.1 N HCl (pH 1.2), and disodium hydrogen phosphate buffer (pH 6.8), at 37°C. The IDRs of all the compounds were estimated on the basis of their individual molar extinction coefficients in the respective medium (Table 4). We noted that the IDR is higher for the first 30 min of the dissolution experiment but the value decreased with time except in a few cases (Table 5). The IDR in water followed the following order: NF–L-arginine–H_2O > NF–PABA > NF β polymorph > NF monohydrate II > NF–urea for the first 30 min and NF–L-arginine–H_2O > NF–PABA > NF β polymorph > NF–urea > NF monohydrate II for 4 h. In 0.1 N HCl, the order is NF–L-arginine–H_2O > NF–PABA > NF–urea > NF β polymorph > NF monohydrate II, and the same trend is observed in pH 6.8 buffer (Fig. 10). The IDR of NF solid forms was higher in buffer solution compared with pure water and the least in acidic medium, indicating that the pH is important in drug dissolution. The role of coformer is important for the dissolution of this free base drug at neutral pH but not so much

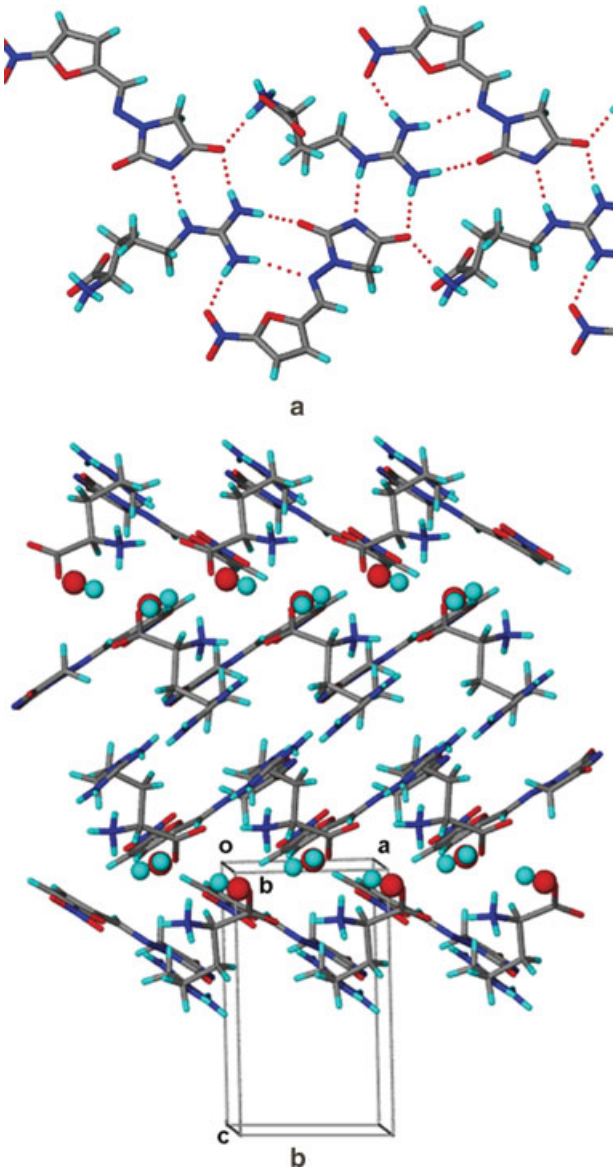

Figure 5. (a) A tape of nitrofurantoin and L-arginine molecules connected by N-H···O and N-H···N two-point motif. (b) Screw-axis related water molecules reside in channels parallel to the *a*-axis and are bonded to NF and L-arginine through O_{water}-H···O_{arg} and $N^{+}{}_{arg}$-H···O_{water} hydrogen bonds and an auxiliary C_{NF}-H···O_{water} interaction.

in acidic conditions. The higher dissolution rate of NF β polymorph than that of NF monohydrate II is consistent with previous reports.[4,7] The IDR of NF–urea cocrystal is closer to both NF β polymorph and NF monohydrate II in the three media. The lower IDR of NF–urea cocrystal is attributed to its faster dissociation and further transformation of unbound NF on the exposed surface of the disk to NF monohydrate II. The same transformation of NF α polymorph to NF monohydrate II during dissolution of the tablet surface was concluded by the observation that the IDRs of the two forms are comparable.[7] The NF–urea cocrystal was partially converted to NF monohydrate

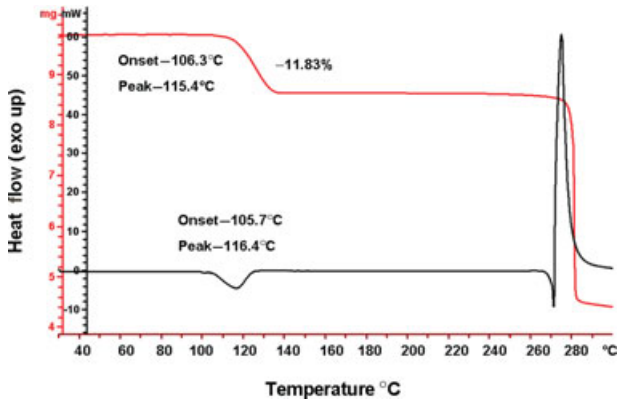

Figure 6. Differential scanning calorimetry (black) and thermogravimetric analysis (red) of nitrofurantoin methanolate. The weight loss is consistent with one mole of MeOH in the solvate structure.

II (see XRPD in Fig. 11) after the dissolution experiment. The NF–PABA cocrystal is stable to hydration in aqueous medium during dissolution (it is stable in water slurry, Fig. 8) but partially converted to NF monohydrate II in 0.1 N HCl and pH 6.8 buffer media (Fig. 12). This difference in physicochemical behavior may be due to change in the ionization state of the components at different acidity levels, resulting in cocrystal dissociation and causing unbound NF to hydrate. The higher IDR of NF–PABA cocrystal compared with that of the NF–urea is attributed to its slower transformation to NF monohydrate II as observed from its higher content in the undissolved material at the end of dissolution experiments. In contrast, NF–L-arginine–H_2O salt completely transformed to NF monohydrate II in dissolution experiments carried out in all the three media (Fig. S5, Supporting Information). The significance of this observation is that it runs contrary to the popular belief that ionic salts are more stable than neutral cocrystals for drug formulation. The neutral NF–PABA cocrystal is more stable in dissolution and slurry experiments in aqueous medium compared with NF–L-arginine–H_2O salt.

CONCLUSIONS

Cocrystallization with a few coformers was evaluated as a pharmaceutical development methodology to control the hydration and dissolution behavior of NF. All the cocrystals/salt except NF–MeOH were found to be stable at ambient temperature and humidity conditions. The two cocrystals NF—PABA and NF–urea come under the category of pharmaceutical cocrystals[18] because of the generally recognized as safe status of the coformers.[27] The NF–urea cocrystal has comparable dissolution profile to that of NF β polymorph and NF monohydrate II. NF–L-arginine–H_2O and NF–PABA have

Table 3. Activity of PABA as an Additive on the Composition of NF–PABA Cocrystal and NF Monohydrate II in Water Slurry Residue, Free NF Transforms to Monohydrate

% of PABA to NF in Crystallization	% of NF–PABA in residue	% of NF Monohydrate II in residue	R_p (%) From XRPD
5	10	90	27.12
10	32	68	26.30
20	48	52	22.42
30	71	29	25.14
40	88	12	32.95
50	92	8	26.15
57.5	100	0	15.63
60	100	0	16.44

NF–PABA, nitrofurantoin–*p*-aminobenzoic acid.

high IDRs compared with the reference drug but NF–L-arginine–H_2O has stability issues because of its facile transformation to NF monohydrate. Among the three adducts, NF–PABA cocrystal is the least susceptible to transformation to NF monohydrate II in aqueous medium and it has good solubility and dissolution rate. The amount of actual drug absorbed can be adjusted by modifying the dosage amount and tablet size. The stability of NF–PABA cocrystal in water slurry suggests its potential utility as a new solid form for controlling drug composition and activity. This limited-scope laboratory study suggests that, in some cases, the relatively new cocrystals methodology may be preferable to the traditional salt forms of drugs for controlling the physicochemical properties of drugs.

Experimental

Materials

Nitrofurantoin was purchased from Alfa Aesar (Hyderabad, Andhra Pradesh, India) and was used without further purification. All other chemicals were of analytical or chromatographic grade. Water filtered through a double-deionized purification system (Milli Q Plus Water System from Millipore Co., Billerica, Massachusetts) was used in all the experiments.

Crystallization of the Molecular Complexes

Nitrofurantoin–p-Aminobenzoic Acid

Nitrofurantoin (23.8 mg, 0.1 mmol) and PABA (13.7 mg, 0.1 mmol) were dissolved in 5 mL hot acetonitrile and left for slow evaporation at room temperature. Brownish red crystals were formed after a few days upon solvent evaporation. The cocrystal has no definite melting point (m.p.) and started to decompose from 210°C (m.p. of NF 263°C, m.p. of PABA 186°C).

Nitrofurantoin–Urea

Nitrofurantoin (46.8 mg, 0.2 mmol) and urea (12 mg, 0.2 mmol) were taken in a mortar–pestle and ground to powder. The powdered mixture was dissolved in 4 mL of hot 1:1 DMF–dioxane solvent mixture and left for slow evaporation at room temperature. Yellow crystals were formed after few days. The cocrystal has

Table 4. Molar Extinction Coefficients of the Compounds in Different Media

Molar Extinction Coefficient mL mg^{-1} cm^{-1}	NF β	NF Monohydrate II	NF–Urea	NF–PABA	NF–L-Arginine–H_2O
Water	73.69	68.31	58.41	46.10	43.56
0.1 N HCl	68.73	61.04	51.02	43.91	37.04
pH 6.8 buffer	71.61	66.70	57.24	44.80	40.85

NF–PABA, nitrofurantoin–*p*-aminobenzoic acid.

Table 5. IDR of the Compounds in Different Media

	Water		0.1 N HCl		pH 6.8 buffer	
Compound	IDR in μg cm^{-2} min^{-1} (for 30 min)	IDR in μg cm^{-2} min^{-1} (for 4 h)	IDR in μg cm^{-2} min^{-1} (for 30 min)	IDR in μg cm^{-2} min^{-1} (for 4 h)	IDR in μg cm^{-2} min^{-1} (for 30 min)	IDR in μg cm^{-2} min^{-1} (for 4 h)
NF β	44.2	37.1	39.7	30.8	48.5	43.4
NF monohydrate II	37.8	33.9	27.3	25.8	47.1	41.3
NF–urea	32.5	36.5	39.9	35.8	51.5	52.2
NF–PABA	58.5	54.4	50.3	44.1	72.2	68.9
NF–L-arginine–H_2O	119.6	107.1	75.9	52.6	138.5	165.5

IDR, intrinsic dissolution rate; NF–PABA, nitrofurantoin–*p*-aminobenzoic acid.

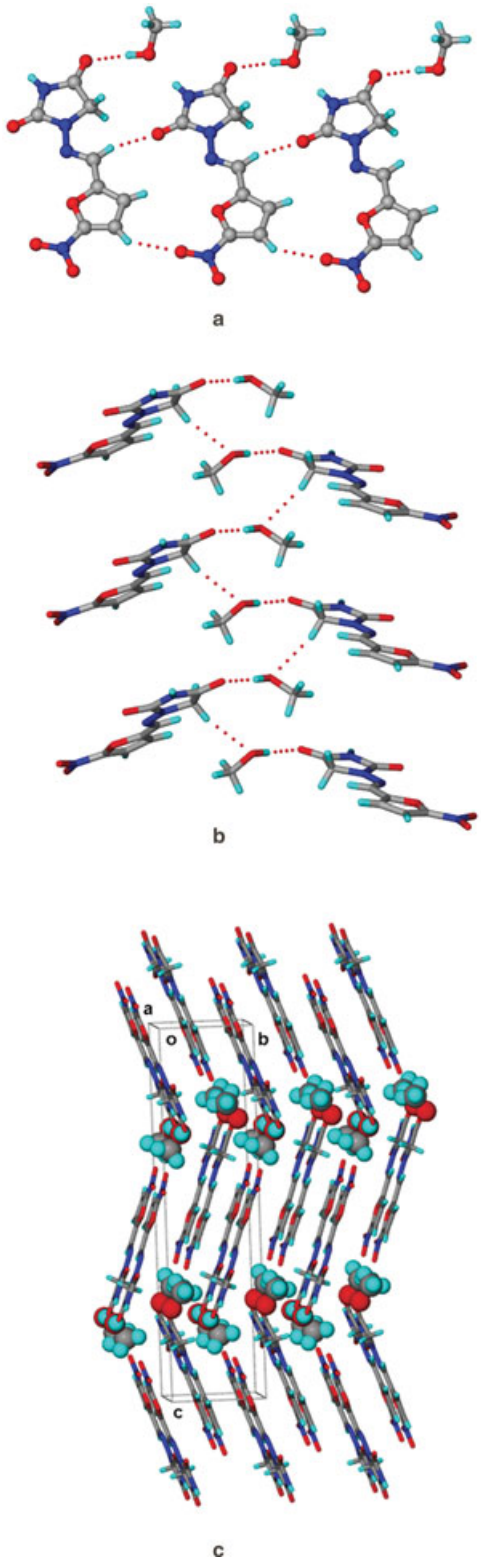

Figure 7. (a and b) A ribbon of nitrofurantoin molecules formed by C-H···O interactions connects the channel of solvent methanol through O_{MeOH}-H···O_{NF} hydrogen bonds along the *a*-axis. (c) Screw-related methanol molecules reside in channels parallel to the *b*-axis, and the overall crystal structure has a herringbone motif.

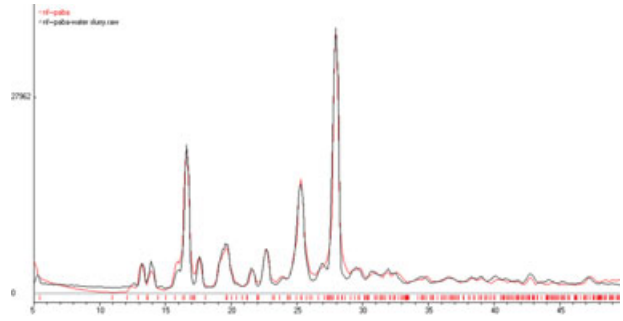

Figure 8. Overlay of the calculated X-ray crystal structure of nitrofurantoin–*p*-aminobenzoic acid (NF–PABA) cocrystal (red) and X-ray powder diffraction pattern of NF—PABA subjected to 3 days stirring in water (black) shows no change.

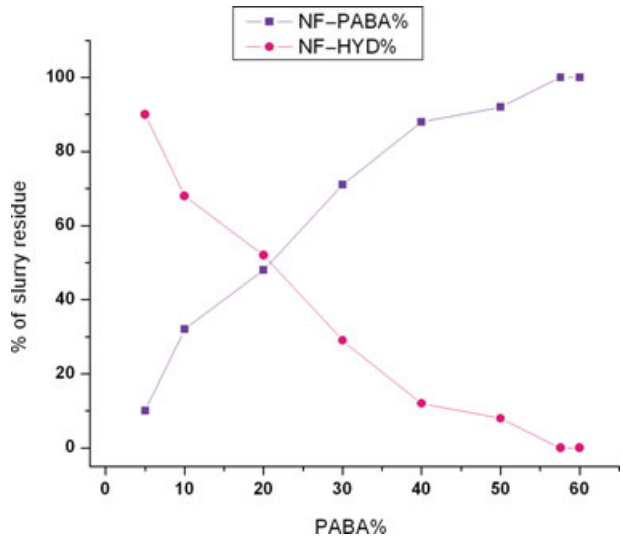

Figure 9. Variation in the composition of nitrofurantoin–*p*-aminobenzoic acid (NF–PABA) cocrystal and NF monohydrate II in the water slurry residue with increase of PABA concentration.

no definite m.p. and it started to decompose at 160°C (m.p. of urea 133°C).

Nitrofurantoin–L–Arginine–H_2O

A powdered mixture of NF (23.8 mg, 0.1 mmol) and L-arginine (17.4 mg, 0.1 mmol) was dissolved in 6 mL of hot 1:1 acetonitrile–isopropanol solvent mixture. Brown crystals of 1:1:1 NF–L-arginine–H_2O were formed after a few days upon solvent evaporation at room temperature. The salt has no definite m.p. and it started to decompose at 170°C (m.p. of L-arginine 222°C).

Nitrofurantoin–MeOH

Fifty milligrams of NF was dissolved in 15 mL of hot MeOH and left for slow evaporation at room temperature. Yellow crystals in equilibrium with the mother

 DOI 10.1002/jps

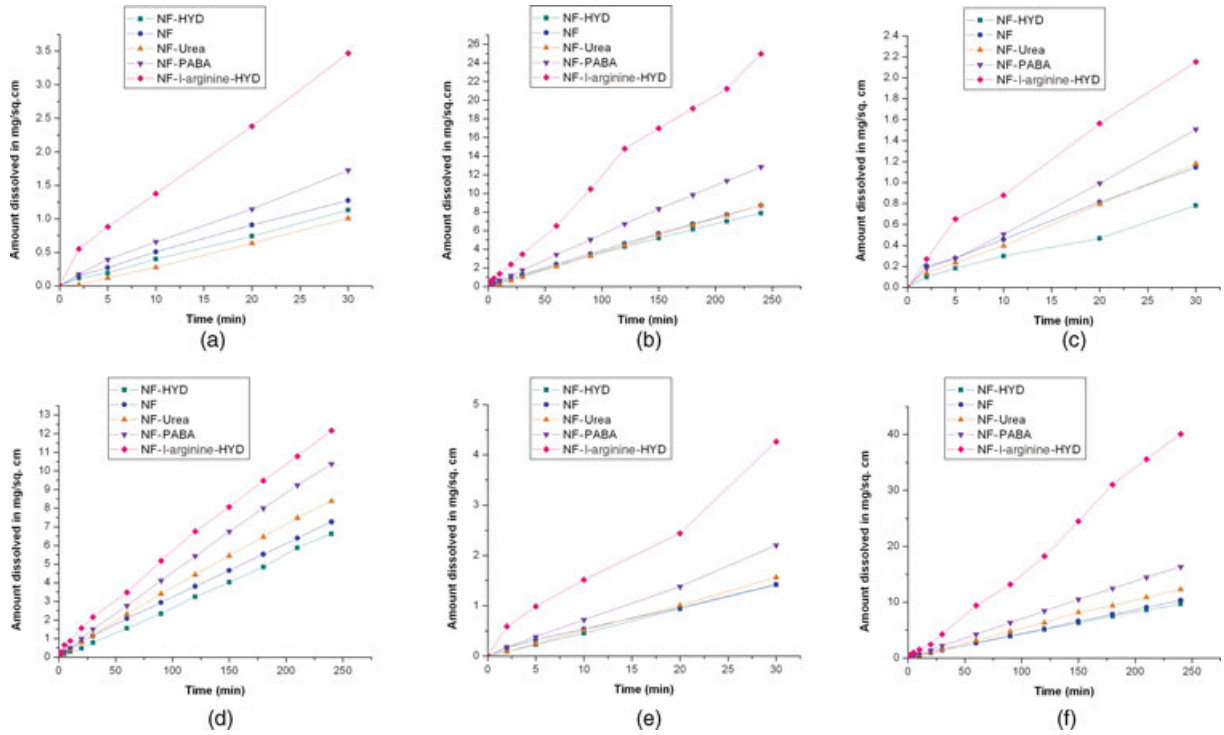

Figure 10. Dissolution profile of nitrofurantoin and its adducts in water (a and b), 0.1 N HCl (c and d), and (e and f) pH 6.8 buffer.

liquor formed after 1 day were filtered and used for characterization.

X-ray Crystallography

X-ray reflections were collected on Bruker SMART-APEX CCD diffractometer (Bruker-AXS, Karlsruhe, Germany). Mo–Kα ($\lambda = 0.71073$ Å) radiation was used to collect X-ray reflections on the single crystal. Data reduction was performed using Bruker SAINT software.[28] Intensities for absorption were corrected using SADABS - Siemens Area Detector ABSorption correction program (Bruker-AXS).[29] Structures were solved and refined using SHELX-97 (Sheldrick GM, Institut Anorg. Chemie, Gottingen, Germany)[30]

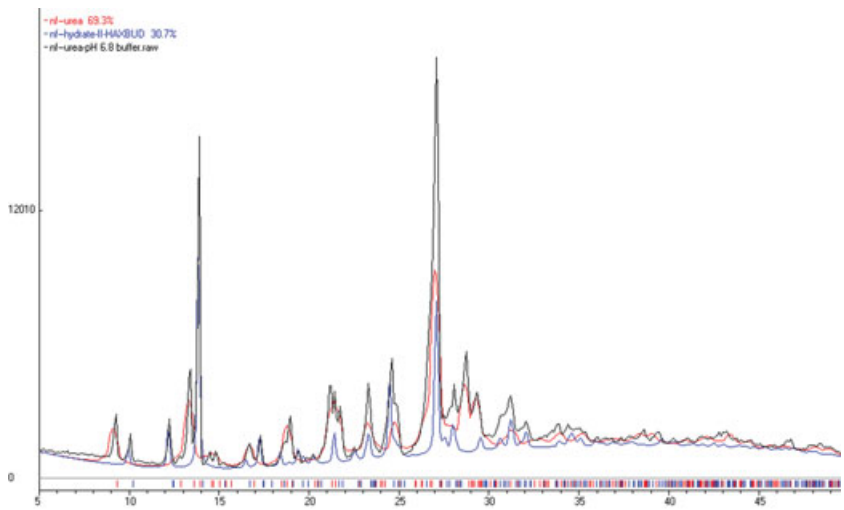

Figure 11. Overlay of the calculated X-ray crystal structures of nitrofurantoin (NF)–urea (red) and NF monohydrate II (blue) on the X-ray powder diffraction pattern of NF–urea cocrystal subjected to dissolution in pH 6.8 buffer (black) shows 70:30 composition by Rietveld refinement ($R_p = 15.14\%$).

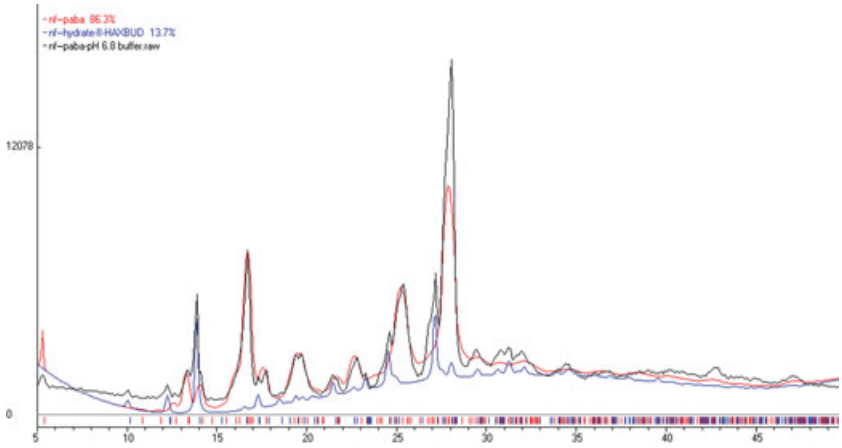

Figure 12. Overlay of the calculated X-ray crystal structures of nitrofurantoin–*p*-aminobenzoic acid (NF–PABA) (red) and NF monohydrate II (blue) on the X-ray powder diffraction pattern of NF–PABA cocrystal subjected to dissolution in pH 6.8 buffer (black) shows 86:14 composition by Rietveld refinement ($R_p = 16.41\%$).

with anisotropic displacement parameters for non-H atoms. Hydrogen atoms on O and N were experimentally located in difference electron density maps. All C-H atoms were fixed geometrically using HFIX command in SHELX-TL (Bruker-AXS).[31] A check of the final CIF file using PLATON (Spek AL, Utrecht University, Utrecht, Netherlands)[32] did not show any missed symmetry. Hydrogen bond distances shown in Table 2 are neutron normalized to fix the D–H distance to its accurate neutron value in the X-ray crystal structures (O–H 0.983 Å, N–H 1.009 Å, and C–H 1.083 Å). X-Seed (Barbour LJ, University of Stellenbosch, Stellenbosch, South Africa)[33] was used to prepare packing diagrams. Crystallographic.cif files (Cambridge Crystallographic Data Centre nos. 797394–797397) are available at http://www.ccdc.cam.ac.uk/data_request/cif.

X-Ray Powder Diffraction

X-ray powder diffraction of all the samples were recorded on Bruker D8 Advance diffractometer (Bruker-AXS) using Cu–Kα X-radiation (λ = 1.5406 Å) at 40 kV and 30 mA. Diffraction patterns were collected over 2θ range of 5°–50° at scan rate of 1 min^{-1}. PowderCell 2.4 (Kraus W & Nolze G, Federal Institute of Materials Research and Testing, Berlin, Germany) was used for Rietveld refinement.[34]

Thermal Analysis

Differential scanning calorimetry was performed on a Mettler Toledo DSC 822e module, and TGA was performed on a Mettler Toledo TGA/SDTA 851e module (Mettler-Toledo Columbus, Ohio). Samples were placed in sealed pin-pricked alumina pans for TG experiments and in crimped but vented aluminum pans for DSC experiments. The typical sample size is 3–5 mg for DSC and 8–12 mg for TGA. Temperature range was 30°C–300°C at heating rate of 5°C/min. Samples were purged by a stream of nitrogen flowing at 80 mL/min for DSC and 50 mL/min for TGA. TG–MS was performed on Netzsch STA 409 PC coupled to Netzsch QMS 403C (Netzsch, Burlington, Massachusetts).

CHN Analysis

Microanalysis was performed on ThermoFinnigan/EA 1112 CHNS analyzer on a 5 mg sample (Thermo Scientific, Brooklyn, New York).

Solubility and Intrinsic Dissolution Measurements

Equilibrium solubility was determined in water using the shake-flask method.[35] One hundred milligrams of powdered compound was added to 5 mL of water, and the resulting suspension was stirred at room temperature for 24 h. The suspension was then filtered through 2.5-μm Whatman filter paper (Whatman India, Mumbai, Maharashtra, India). The concentration of the solution thus obtained was determined on a Thermo Scientific Evolution 300 UV–Vis spectrometer (Thermo Scientific, Waltham, Massachusetts) based on the absorbance at 368 nm (λ_{max} of NF devoid of interference from other compounds) with appropriate dilution using a predetermined standard curve. Intrinsic dissolution experiments in water, 0.1 N HCl, and pH 6.8 buffer were carried on a USP certified Electrolab TDT-08L Dissolution Tester (Electrolab, Mumbai, Maharashtra, India) for 4 h. The pH 6.8 buffer was prepared as per the International Pharmacopoeia (3rd ed., 2003).[36] Prior to IDR estimation, standard curves of all the compounds in the three media were obtained spectrophotometrically at 368 nm. The respective molar extinction coefficients were used to determine the IDR. For IDR testing, 100 mg of the compound was taken in the intrinsic attachment and

compressed to a 0.5 cm^2 disk using a hydraulic press at a pressure of 2.5 ton/$in.^2$ for 5 min. The intrinsic attachment was placed in a jar of 500 mL medium preheated to 37°C and rotated at 150 rpm. Five milliliter aliquots were collected at specific time intervals, and concentration of the aliquots were determined with suitable dilution from the predetermined standard curves of the respective compounds. The linear region of the dissolution profile (regression >0.99) was used to determine the IDR of the compound as (slope of the amount dissolved divided by surface area of the disk) per unit time. The identity of the undissolved materials after solubility and dissolution experiments was established through XRPD. There is no transformation of the compounds upon compression as analyzed by XRPD.

ACKNOWLEDGMENTS

S. Cherukuvada and N. Jagadeesh Babu thank the Indian Council of Medical Research and University Grants Commission (UGC) for fellowship. We thank the Department of Science and Technology (DST; grant numbers SR/S1/OC-67/2006 and SR/S1/RFOC-01/2007), Govt. of India, and Council of Scientific & Industrial Research [CSIR; grant number 01(2079)/06/EMR-II], India, for research funding and DST (Intensification of Research in High Priority Areas grant) and UGC (Promotion of University Research and Scientific Excellence grant) for providing instrumentation and infrastructure facilities.

REFERENCES

1. Miller-Hjelle MA, Somaraju V, Hjelle JT. 1997. In Modern pharmacology with clinical applications; Craig CR, Stitzel RE, Eds. 5th ed. Boston: Little Brown & Company, pp 515–525.
2. WHO model list of Essential Medicines. http://www.who.int/selection_medicines/committees/expert/17/sixteenth_adult_list_en.pdf last accessed March 10th 2011.
3. Marshall PV, York P. 1989. Crystallization solvent induced solid-state and particulate modifications of nitrofurantoin. Int J Pharm 55:257–263.
4. Otsuka M, Teraoka R, Matsuda Y. 1991. Physicochemical properties of nitrofurantoin anhydrate and monohydrate and their dissolution. Chem Pharm Bull 39:2667–2670.
5. Pienaar EW, Caira MR, Lötter AP. 1993. Polymorphs of nitrofurantoin. 2. Preparation and X-ray crystal structures of two anhydrous forms of nitrofurantoin. J Crystallogr Spectr Res 23:785–790.
6. Pienaar EW, Caira MR, Lötter AP. 1993. Polymorphs of nitrofurantoin. 1. Preparation and X-ray crystal structures of two monohydrated forms of nitrofurantoin. J Crystallogr Spectr Res 23:739–744.
7. Caira MR, Pienaar EW, Lötter AP. 1996. Polymorphism and pseudopolymorphism of the antibacterial nitrofurantoin. Mol Cryst Liq Cryst 279:241–264.
8. Kasim NA, Whitehouse M, Ramachandran C, Bermejo M, Lennernas H, Hussain AS, Junginger HE, Stavchansky SA, Midha KK, Shah VP, Amidon GL. 2004. Molecular properties of WHO essential drugs and provisional biopharmaceutical classification. Mol Pharm 1:85–96.
9. Paul HE, Kenyon JH, Paul MF, Borgmann AR. 1967. Laboratory studies with nitrofurantoin. Relationship between crystal size, urinary excretion in the rat and man, and emesis in dogs. J Pharm Sci 56:882–885.
10. http://www.pfizer.com.au/ProductInfo.aspx.
11. Tian F, Qu H, Louhi-Kultanen M, Rantanen J. 2009. Mechanistic insight into the evaporative crystallization of two polymorphs of nitrofurantoin monohydrate. J Cryst Growth 311:2580–2589.
12. Sandler N, Rantanen J, Heinämäki J, Römer M, Marvola M, Yliruusi J. 2005. Pellet manufacturing by extrusion-spheronization using process analytical technology. AAPS PharmSciTech 6:E174–E183.
13. Wikström H, Rantanen J, Gift AD, Taylor LS. 2008. Toward an understanding of the factors influencing anhydrate-to-hydrate transformation kinetics in aqueous environments. Cryst Growth Des 8:2684–2693.
14. Koradia V, Diego HLD, Elema MR, Rantanen J. 2010. Integrated approach to study the dehydration kinetics of nitrofurantoin mononhydrate. J Pharm Sci 99:3966–3976.
15. Otsuka M, Teraoka R, Matsuda Y. 1992. Rotating-disk dissolution kinetics of nitrofurantoin anhydrate and monohydrate at various temperatures. Pharm Res 9:307–311.
16. Gever G, Vincent JG. 1962. Improvements in or relating to nitrofurantoin salts. PatentGB 902692, PatentUS 3007846.
17. Deboeck AM, Fossion JJ, Smolders RR. 1982. Nitrofurantoin salts, their preparation and their useSels de nitrofurantoine, leur preparation et leur utilization. European Patent 0066934.
18. Shan N, Zaworotko MJ. 2008. The role of cocrystals in pharmaceutical science. Drug Discov Today 13:440–446.
19. Childs SL, Zaworotko MJ. 2009. The reemergence of cocrystals: The crystal clear writing is on the wall. Introduction to virtual issue on pharmaceutical cocrystals. Cryst Growth Des 9:4208–4211.
20. Stanton MK, Kelly RC, Colletti A, Kiang YH, Langley M, Munson EJ, Peterson ML, Roberts J, Wells M. 2010. Improved pharmacokinetics of AMG 517 through co-crystallization Part 1: Comparison of two acids with corresponding amide cocrystals. J Pharm Sci 99:3769–3778.
21. Karki S, Friščić T, Fábián L, Laity PR, Day GM, Jones W. 2009. Improving mechanical properties of crystalline solids by cocrystal formation: New compressible forms of paracetamol. Adv Mater 21:3905–3909.
22. Trask AW, Motherwell WDS, Jones W. 2005. Pharmaceutical cocrystallization: Engineering a remedy for caffeine hydration. Cryst Growth Des 5:1013–1021.
23. Desiraju GR. 1995. Supramolecular synthons in crystal engineering—A new organic synthesis. Angew Chem Int Ed Engl 34:2311–2327.
24. Walsh RDB, Bradner MW, Fleischman S, Morales LA, Moulton B, Rodríguez-Hornedo N, Zaworotko MJ. 2003. Crystal engineering of the composition of pharmaceutical phases. Chem Commun 2:186–187.
25. Byrn SR, Pfeiffer RR, Stowell JG. 1999. Solid-state chemistry of drugs. 2nd ed. West Lafayette, Indiana: SSCI, Inc., pp 233–247.
26. Shan N, Toda F, Jones W. 2002. Mechanochemistry and cocrystal formation: Effect of solvent on reaction kinetics. Chem Commun 20:2372–2373.
27. GRAS chemicals list. http://www.fda.gov/Food/FoodIngredientsPackaging/ucm115326.htm.
28. SAINT-Plus, version 6.45. 2003. Madison, Wisconsin: Bruker AXS Inc.
29. Sheldrick GM. 1997. SADABS, Program for Empirical Absorption Correction of Area Detector Data. Göttingen, Germany: University of Göttingen.

30. Sheldrick GM. 1997. SHELXS-97 and SHELXL-97, Göttingen, Germany:University of Göttingen.
31. SMART (Version 5.625) and SHELX-TL (Version 6.12). 2000. Madison, Wisconsin: Bruker AXS Inc.
32. Spek AL. 2002. PLATON, a multipurpose crystallographic tool. Utrecht, Germany: Utrecht University.
33. Barbour LJ. 1999. X-Seed, Graphical interface to SHELX-97 and POV-Ray. Missouri: University of Missouri-Columbia.
34. PowderCell, a program for structure visualization, powder pattern calculation and profile fitting, http://www.ccp14.ac.uk/tutorial/powdercell
35. Glomme A, Marz J, Dressman JB. 2005. Comparison of miniaturized shake-flask solubility method with automated potentiometric acid/base titrations and calculated solubilities. J Pharm Sci 94:1–16.
36. The International Pharmacopoeia. 3rd ed. Geneva:WHO; 2003.